INJ INTERNATIONAL NEUROUROLOGY JOURNAL

An Improved Denoising Auto-Encoder Deep Learning High Boost Filter for Restoration and Enhancement of Rician corrupted Brain MR Images

M.S.Bhuvaneswari[1], N.Bala Ganesh[2*]
Assistant Professor, Department of Smart Computing, School of Computer Science Engineering and Information Systems, Vellore Institute of Technology, Vellore, Tamil Nadu, 632014, India
Assistant Professor, Department of Software and Systems Engineering, School of Computer Science Engineering and Information Systems, Vellore Institute of Technology, Vellore, Tamil Nadu, 632014, India

Abstract

Magnetic resonance imaging is the clinically acclaimed imaging modalities which is utilized for the screening of brain abnormalities. It provides the visual interpretation of the abnormalities in terms of tumors, masses, grey matter and clots. However, these readable features of brain are affected due to the presence of inherent Rician noise. Moreover, it also restricts the decision capability of the expert about the brain abnormalities. So, for the restoration and enhancement the brain MR images, an improved denoising auto encoder high boost filter i.e., IDAEHBF is proposed. In order to develop the proposed IDAEHBF, the smoothening filter of high boost is swapped with the improved denoising auto encoder i.e., IDAE. Furthermore, the symmetry skip connection has been used in the conventional denoising auto encoder to form the IDAE. This modification provides a better correlation amid the noisy pixel and encoder-decoder part. The efficacy of the proposed method has been assessed with respect to the qualitative and quantitative assessment for the brain web dataset. The human visual system, full and no reference image metrics are used to quantitatively measure the performance of the proposed method. Apart from this, a comparative study has been also presented between the proposed and existing method to describe the effectiveness of the proposed method. The obtained results demonstrate that the proposed method is capable of simultaneously reducing Rician noise, preserving edges, restoring fine details, and enhancing anomalies.

Key Words: Brain, Magnetic Resonance Imaging, Denoising Auto-Encoder, Enhancement, High Boost, Restoration.

Introduction

The brain screening provides the structural overview as well as changes in the brain functionality [1]. It describes the brain disorder and conditions in terms of abnormalities such as grey matter particles, tumors, clots and masses. Epilepsy, schizophrenia, autism, Parkinson's, stroke, and dementias are the most common types of neurological illnesses affecting the brain [2]. These disorders are raised due the alteration in the shape of brain cells. The incidence and mortality rate by of brain disorder are increasing day to day. It can be only prevented by the early diagnosis of the disorder.

Magnetic resonance imaging (MRI) is the widely used imaging tool for the diagnosis of brain disorders[3]. It is popular due to its non-invasive property and less radiative nature. It concurrently uses a magnetic field and radio waves simulated via computer to obtain the raw images of brain cells. The produced raw images are complex-valued in nature and for the better visualization it is transformed into the magnitude valued image with the aid of mathematical operations [4]. However, the acquired images have low signal-to-noise-ratio that confirms the existence of noise in the image. The origin of noise varies from one source to other. The prominent sources of noise include machine's calibration, sensors, coils, environment illumination, acquisition, transmission, and storage medium [5]. Literature shows that the MR magnitudes image generally comply to the Rician noise [6,7]. It is an undesired inherent characteristic of the image which is multiplicative in nature. It affects both the image's readability features and clarity of the image. It confines the exact interpretation of the diseases by the experts. Moreover, it reduces the high frequency as well as the fine detail information of the image such as edges and boundary. Thus, the brain image restoration and enhancement are the two major concern that should be addressed properly for the early diagnosis of brain disorder.

To achieve the restoration and enhancement of brain MR images in a single framework, an improved denoising auto encoder deep learning based high boost filter (IDAEHBF) has been proposed. It combines the attributes of denoising auto-encoder (DAE) [8] and high boost filter (HBF) [9] for the image denoising and quality improvement respectively. The development of the proposed IDAEHBF begins with the swapping of smoothening filter of high boost with the improved denoising auto encoder (IDEA). It is the first advancement and it offers a better denoised-smoothen image of the noisy image. Furthermore, in the second advancement the

ISSN:2093-4777 | E-ISSN:2093-6931
DOI: 10.5123/inj.2023.4.in82
Vol. 27 Iss. 4 (2023)

efficacy of conventional denoising auto encoder (CDAE) has been refined with the help of the symmetry skip connection [10] in order to form the IDAE. It provides a better correlation between the noisy pixel data with the layers of auto encoder-decoder model.

The rest of the paper has been systematized as follows: section 2 reports the literature of existing denoising methods in contrast to MRI images. Section 3 illustrates about the used dataset and the proposed methodology. Section 4 presents the information of the performance assessment metrics in terms of human visual system, full and no reference image metric. Section 5 describes the performance of the proposed IDAEHBF. And, section 6 presents an overall conclusion.

Literature Survey

There has been various method developed to alleviate the negative impact of the Rician noise. It skews the exact position of brain lesions and makes medical diagnosis less precise. The denoising approaches for Rician noise have been widely classified as spatial, transform, similarity, and partial differential equation (PDE) based filters [11]. The mostly used spatial domain-based filter are median and wiener filter respectively. Gabor filter [6] and wavelet method lies under the transform domain denoising filter. The similarity based denoising filters comprises non-local means [12] and its modified form [13]. Furthermore, PDE-based techniques for MRI image denoising include total variation [14], anisotropic diffusion [15], complex diffusion [16,17], and fourth order partial differential equation [18]. Apart from this, some of the methods follows the image enhancement after the image denoising.

Lee et al. [19] had used the properties of median and wiener filter for the denoising of T1 weighted brain MR images of the brain web dataset. The performance was illustrated with correspond to qualitative and quantitative assessment such as edge preservation index and coefficient of variation. Redhya et al. [20] had utilized adaptive median filter to minimize the noise from brain MR images. The work was primarily developed for the classification of Parkinson diseases. The image quality assessment parameters like mean square error (MSE), image enhancement factor and peak-signal-to-noise-ratio (PSNR) were estimated to judge the effectiveness of the method. Singh et al. [21] had compared the performance of median, gaussian and wiener filter for the denoising of brain MR images. The efficacy was judged with respect to MSE and PSNR image metric. Ali et al [22] had employed mixing concatenation residual network (MCR) for the gaussian and salt-pepper noise elimination from brain MR images. In this method six consecutive convolutional layers with the rectified linear unit (ReLU) were used for the denoising of image. The metrics such as structural similarity index map (SSIM), PSNR and SSIM was determined as image quality assessment parameters. Kumar et al. [12] had clubs the PDE based anisotropic diffusion and unsharp masking for the noise removal of brain MR images. The method effectiveness was judged for MSE, PSNR, SSIM, correlation parameter (CP), and blind reference image spatial quality evaluator respectively. Yadav et al. [18] had used the other PDE rooted method i.e., complex diffusion for the elimination of Rician noise from MR images. In this method the image was treated as a complex-valued object, where the real and imaginary parts correspond to the intensity and gradient of the image respectively. The method efficacy was estimated for brain-web dataset and the metrics such MSE, PSNR, CP and SSIM were used for assessment purpose. Zhang et al. [14] had employed total-variation for the restoration of brain MR images. The method combines Fischer Burmeister function to regularize the total variation. The method effectiveness was evaluated in terms of MSE, PSNR and SSIM. Thakur et al. [23] had compared the working capability of denoising filters such as NLM, block matching three-dimensional filter, weighted nuclear norm minimization and fast Fourier transform. All of these approaches were tested on MR images and assessment metrics like PSNR and SSIM were analyzed. Kollem et al. [24] had used FPDE and quaternion wavelet transform for the noise removal from the MR images. The method uses a diffusivity function to advance the characteristic of PDE. PSNR, SSIM and MSE were evaluated to measure the performance of the method. Dinh [25] had combined the attributes of contrast limited adaptive histogram equalization, denoise convolutional neural network, Laplacian edge detector and marine predators' algorithm respectively for the removal of noise and enhancement of medical image. The method effectiveness was determined in terms of entropy, average gradient, and mean light intensity. Kumar et al. [6] had applied a reshaped Gabor filter for the denoising of MR images. The qualitative as well as quantitative assessment was performed to measure the efficacy of method.

The method such as ADF [15], and MCD [16] have an issue of over smoothening which obscures fine details. The method based on ADMF [20], WF [21], MCR [22], and Gabor [6] produces a low contrast image and fails to eliminate the noise. Furthermore, the methods like FPDE[18], NLM [23] and TV [14] have limited performance in contrast to edge or high frequency information preservation. Thus, the main drawbacks of the current approaches can be understood from the reported literature in terms of excessive smoothing, edge blurring, loss of high frequency information and the formation of low contrast images. Therefore, an improved

ISSN:2093-4777 | E-ISSN:2093-6931
DOI: 10.5123/inj.2023.4.in82
Vol. 27 Iss. 4 (2023)

denoising auto encoder deep learning based high boost filter (IDAEHBF) has been presented to address these key problems. The major contributions of the proposed IDAEHBF are as follows:

1) It proposes a method that clubs the features of high boost filter (HBF) and denoising auto-encoder (DAE) in a single framework for the restoration and enhancement of Rician corrupted brain MR image.
2) It presents an improved denoising auto-encoder (IDAE) at the place of the smoothen low pass function in high boost to readdress the restrictions of HBF.
3) To refine the efficacy of conventional DAE (CDAE) a modification has been employed. To add encoder and decoder layers, symmetry skip connections are fabricated. This modification offers a better learning and visualization of noisy pixels.
4) The proposed IDAEHBF has been validated on T1, T2 and PD weighted MRI images of brain web dataset.

Research Methodology

The restoration and enhancement of Rician impacted brain MR images, an improved denoising auto encoder deep learning based high boost (IDAEHBF) has been proposed. The collection of MR brain images is the first steps in the development of the proposed method. The IDAEHBF utilizes the features of conventional denoising auto encoder (CDAE) and high boost filter (HBF). The function of CDAE is to eliminate the noise from the images while a HBF is utilized for image enhancement. To increase the robustness of the HBF, the IDAE is substituted at the place of low-pass module in HBF. This modification provides a better denoised image in compare to the conventional low-pass approach. However, the CDAE have some limitations in terms of gradient flow, multi-scale feature learning and mitigating information loss. So, to refine the performance of CDAE a symmetry skip connection is added amid the layers of encoder and decoder part. Figure 1 shows the block diagram of the proposed IDAEHBF.

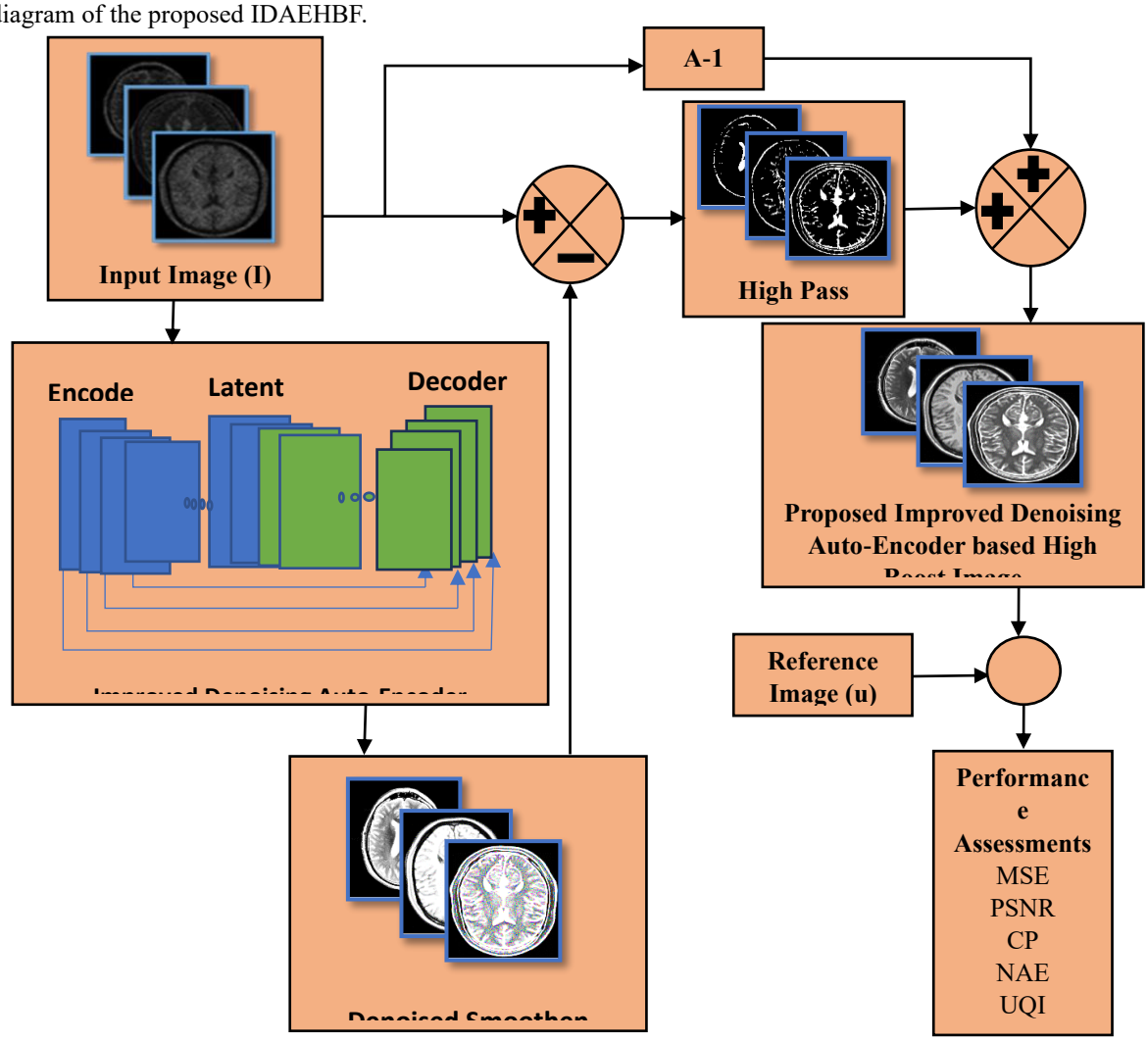

Figure 1: Flowchart of the proposed improved denoising auto encoder deep learning high boost filter

DOI: 10.5123/inj.2023.4.in82
ISSN:2093-4777 | E-ISSN:2093-6931
Vol. 27 Iss. 4 (2023)

Dataset Collection

To develop the proposed method IDAEHBF, brain web [26] dataset has been collected. It is an openly accessible database that is used as a benchmark data for the research work. The complete description of the database is given in Table 1.

Table 1: Information of the Brain Web Database

Key	Description
Imaging modalities	T1, T2, and PD
Types of noise variance	0%, 3%, 5%, 7% and 9%
Total Number of images	905 for each imaging modality
Image storage format	Portable Network Graphics (PNG)
Accessibility	Publicly
Size of image	181×127 Pixel

Proposed Improved Denoising Auto Encoder Deep Learning High Boost Filter

MRI screening provides information in the form of raw image data, which is primarily a complex valued data. These raw image data are converted into magnitude MR valued images for simple interpretation. However, the images are get affected by noise during the image acquiring, transmitting and storing respectively. It restricts the effectiveness of qualitative and quantitative measurements derived from MR images. The MRI image's general form [27] can be represented as:

$$g = m * h + a \quad (1a)$$
$$g = Rician * h + a \quad (1b)$$

where h is the MRI image affected by Rician noise, a is the additive noise, and g is the magnitude MRI image. For the development of the method, additive noise is neglected. Let the digitized form of magnitude MR image is expressed by I then its the probability distribution correspond to Rician noise [16] may read as:

$$P(M,\sigma) = \frac{M}{\sigma^2} exp\ exp\left[\frac{I^2+M^2}{2\sigma^2}\right] J_o\left(\frac{IM}{\sigma^2}\right) H(M) \quad (2)$$

where, I represent the amplitude of the noiseless image, σ^2 is the variance, $J_o(.)$ is a first-order modified Bessel function with zero order, $H(.)$ is the unit step Heaviside function, and M is the magnitude of image. In order to restore the image information, improved denoising auto encoder has been employed. The IDAE is a modified form of conventional denoising auto encoder (CDAE) [8]. The CDAE uses a stochastic approach to reconstruct the noisy image. It comprises encoder, latent space and decoder. The encoder takes the input noisy image and maps it to a lower-dimensional representation. Moreover, this lower-dimensional representation is usually referred to as the latent space. The latent space captures the underlying structure of the image while filtering out the noise. Later, the decoder takes the code produced by the latent space and attempts to reconstruct the denoised image using lower dimensional representation of the noisy image.

Let's $\hat{I}$ is noisy input image and the encoder function as E. The encoder maps the noisy input image I to a lower-dimensional representation Z with the aid of the latent space. The overall process may read as:

$$Z = E(\hat{I}) \quad (3)$$

Equation 3, shows the conversion of noisy image into its lower dimensional form. Further, these lower dimensional data is processed by decoder D in order to achieve the reconstructed denoised image. The above statement mathematically governed as:

$$I_{reconstruted/denoised} = D(\hat{I}) \quad (4)$$

The loss function quantifies the discrepancy between the reconstructed data $I_{reconstruted/denoised}$ and the noise free reference image u. MSE loss is a commonly used choice for DAEs:

$$MSE_{Loss} = \frac{1}{MN}\sum_{i=0}^{M-1}\sum_{j=0}^{N-1}[u - I_{reconstruted/denoised}]^2 \quad (5)$$

DOI: 10.5123/inj.2023.4.in82
ISSN:2093-4777 | E-ISSN:2093-6931
Vol. 27 Iss. 4 (2023)

However, the performance of CDAE is limited with respect to the gradient flow and loss function. The refine the efficacy of CDAE, the symmetry skip connection has been incorporated between the layers of encoder and decoder. Figure 2 shows the architecture of proposed IDAE with symmetry skip connection [10]. It allows information from one layer to be directly fed into a later layer of the network, bypassing some intermediate layers. By adding skip connections, the model can have access to both the high-level feature representations learned in the encoder and the low-level details present in the input image. It enhances the model's ability to reconstruct the original denoised image more accurately.

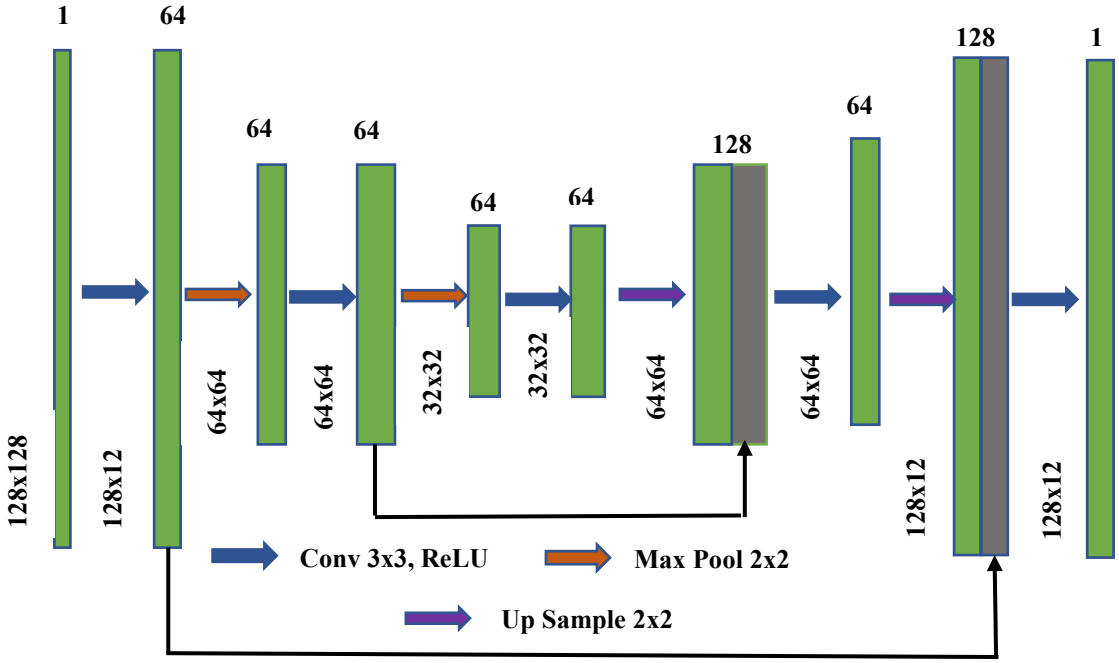

Figure 2: Proposed Improved Denoising Auto-Encoder

The image obtained by IDAE is a low contrast image. So, to boost the image quality IDEA is used as a low pass operator (LPO) in HBF [9]. This idea is incorporated due the limitation of LPO of conventional HBF such as image denoising, edge restoration and fine details preservation respectively. Moreover, this modification also offers an absolute image quality improvement. Thus, all the three process i.e., denoising, restoration and enhancement of the image occurs in a single framework. To ease the implementation let's $I_{IDAE} = I_{reconstruted/denoised}$; where I_{IDAE} is resultant image. The process of creation of IDAEHBF initiates with substituting the IDAE at the place of LPO of conventional HBF. It may define as:

$$I_{LPO} = I_{IDAE} \qquad (6)$$

where, I_{LPO} is the low pass image of HBF; I_{IDAE} is the reconstructed denoised image obtained by proposed IDAE as mentioned in equation 4. To produce the high pass image via HBF process, the resulting image of I_{IDAE} has been subtracted from the input image I. It is mathematically expressed as:

$$I_{HPIDAE} = I - I_{IDAE} \qquad (7)$$

where, I_{HPIDAE} is high pass form of input image I. The high pass form of an image shows the details of image's edges and boundaries. Furthermore, to estimate the high boost form of the image, the scaled version of the input image is added with the resultant image of I_{HPIDAE}. It is expressed as:

$$I_{IDAEHBF} = (A-1).I + I_{HPIDAE} \qquad (8)$$

where, $I_{IDAEHBF}$ is the high boost image of the input image I. It also illustrates the resorted, denoised and enhanced form of the input image, so for simplicity it may denoted as: $I_{IDAEHBF} = I_{RDE}$. Furthermore, A is the amplification factor [28]. It controls the amount of boosting and it should be a positive number where $(A >)$]. Table 2 shows the pseudo code of the proposed improved denoising auto encoder high boost filter.

Table 2: Pseudo code of proposed IDAEHBF

Input: $\{u(i,j),\ I(i,j)\}$, where $I(i,j)$ and $u(i,j)$ are noisy and reference image respectively
Start Computation: Step 1: Give the input image $I(i,j)$ to start the computation process. Step 2: Compute the reconstructed denoised image via improved denoising auto encoder (IDEA) i.e., equation (4) $$I_{reconstruted/denoised} = D(\hat{I})$$ Step 3: Substitute the IDEA as a low pass operator in high boost filter (HBF) and compute the high pass image using equation (6) and (7) respectively $$I_{LPO} = I_{IDAE}$$ and, $I_{HPIDAE} = I - I_{IDAE}$ Step 4: Compute the high boost image using equation (8) as: $$I_{IDAEHBF} = (A-1).I + I_{HPIDAE}$$ Step 5. Evaluate performance metrics. Step 6. Store the result End Computation
Output: $\{I_{IDAEHBF}(i,j)\}$, where $I_{IDAEHBF}(i,j)$ is improved denoising auto encoder high boost image

Performance Evaluation Metrics

The proposed IDAEHBF's efficacy has been measured using multiple performance evaluation metrics. The metrics are divided with respect to human visual system [29], full and no reference [30] image quality assessment measures. Table 5 depicts the mathematical formulation of the measures used.

Table 5: Performance Evaluation Metrics

	Metrics	Mathematical Notation
Full reference Assessment Parameters (FRAP) [30]	Mean-Squared Error (MSE)	$MSE = \frac{1}{MN}\sum_{i=0}^{M-1}\sum_{j=0}^{N-1}[u(i,j) - I_{RDE}(i,j)]^2$
	Peak Signal-to-Noise Ratio (PSNR)	$PSNR = 10\frac{(L-1)}{MSE}db$
	Correlation Parameter (CP)	$CP = \frac{\sum (u(i,j)-\mu_u)\sum (I_{RDE}(i,j)-\mu_{I_{RDE}})}{\sqrt{\sum (u(i,j)-\mu_u)^2 \sum (I_{RDE}(i,j)-\mu_{I_{RDE}})^2}}$
	Normalized Absolute Error (NAE)	$NAE = \frac{\sum_{i=0}^{M-1}\sum_{j=0}^{N-1}\lvert u(i,j) - I_{RDE}(i,j)\rvert}{\sum_{i=0}^{M-1}\sum_{j=0}^{N-1} u(i,j)}$
Human visual system Assessment Parameters (HVSAP) [29]	Universal Quality Index (UQI)	$UQI = \frac{4\mu_u\mu_{I_{RDE}}\sigma_{uI_{RDE}}}{(\mu_u{}^2 + \mu_{I_{RDE}}{}^2)(\sigma_u{}^2 + \sigma_{I_{RDE}}{}^2)}$ here, $\sigma_{uI_{RDE}} = \frac{1}{MN-1}\sum_{i=0}^{M-1}\sum_{j=0}^{N-1}(u(i,j)-\mu_u)(I_{RDE}(i,j)-\mu_{I_{RDE}})$
	Structural Similarity Index (SSIM)	$SSIM = \frac{(2\mu_u\mu_{I_{RDE}} + C_1)(2\sigma_{uI_{RDE}} + C_2)}{(\mu_u{}^2 + \mu_{I_{RDE}}{}^2 + C_1)(\sigma_u{}^2 + \sigma_{I_{RDE}}{}^2 + C_2)}$
No reference Assessment Parameters (NRAP) [30]	Perceptual Sharpness Index (PSI)	$I_{PSI}(i,j) = \{\frac{I_{up}(i,j) - I_{down}(i,j)}{cos\ cos\ (\Delta\emptyset(i,j))} - \frac{I_{max}(i,j) - I_{min}(i,j)}{I(i,j)};\ if\ \frac{I_{up}(i,j) - I_{down}(i,j)}{cos\ cos\ (\Delta\emptyset(i,j))} \geq I_{jnb}\ \frac{I_{up}(i,j) - I_{down}(i,j)}{cos\ cos\ (\Delta\emptyset(i,j))}; otherwise$

Where u and I_{RDE} are the reference image and resultant image of IDEAHBF respectively. σ^2 and μ are the variance and mean of the corresponding image.

Results and Discussion

The performance of the proposed IDSEHBF has been evaluated in terms of qualitative and quantitative assessments. The investigation has been evaluated for T1, T2 and PD weighted brain images of the Brain Web MRI database [26]. Apart from this, a comparative performance study with respect to qualitative and quantitative analysis has been also presented between the proposed and existing methods. For the performance purpose the value of A in HBF has been taken 5.

Qualitative assessment:

The improvement in image quality is measured with the aid of qualitative analysis. To perform the analysis T1, T2 and PD MRI images has been used with respect to the 9% noise variance. However, the process of evaluation stands same for the other noise variances such as 3%, 5%, and 7% of T1, T2 and PD brain MR images.

Figure 3 exhibits the result of all steps involved during the implementation of proposed IDAEHBF for T1 MRI brain images. It comprises of total three images where (a) correspond to sample image; (b) is the noisy form of the sample image; and (c) is the restored, denoised and enhanced image obtained by the proposed method. Furthermore, Figures 4 demonstrates the qualitative result for T2 weighted MR image with 9% noise variance. The very first image i.e., (a) refers to sample input image; the second image i.e., (b) is the noisy image; and the last image i.e., (c) is the restored, denoised and enhanced image attained by the proposed IDAEHBF. In similar way, figure 5 exhibits the qualitative result for PD weighted MR image with 9% noise variance. The image (a) refers to sample input image; the image (b) is the noisy image; and the last image (c) is the restored, denoised and enhanced image attained by the proposed method. Figure 6 shows the illustrative comparative qualitative assessment. The comparison is evaluated with 9% noise variance of T1 MRI brain image. In these figures, image (a) to (i) are the resultant images of FPDE[18], NLM [23], WF [21], MCD [16], TV [14], ADMF [20], MCR [22], ADF [15], Gabor [6] and Proposed IDAEHBF respectively.

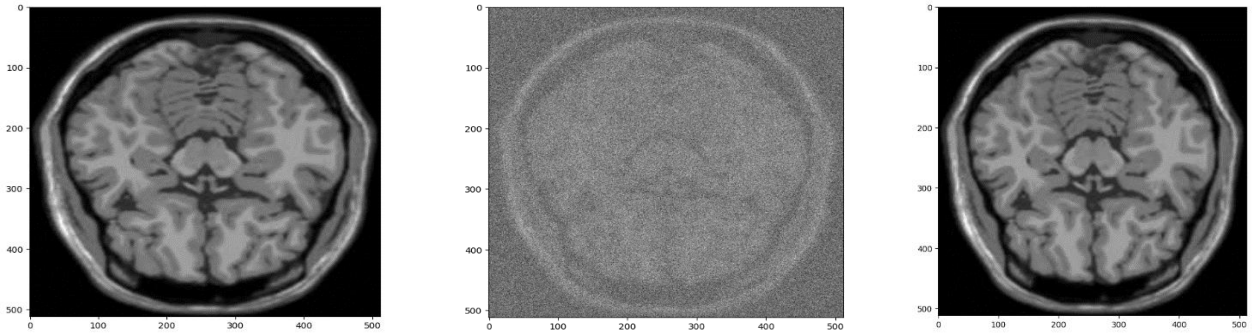

(a) **(b)** **(c)**

Figure 3: Result of proposed method for T1 weighted MR image (a) Noiseless image (b) Noisy Image (c) Output image IDEAHBF

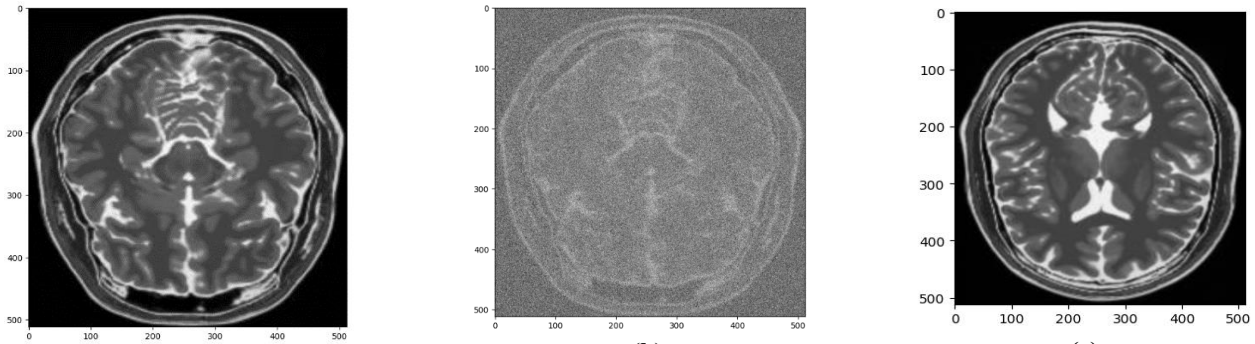

(a) **(b)** **(c)**

Figure 4: Result of proposed method for T2 weighted MR image (a) Noiseless image (b) Noisy Image (c) Output image by IDEAHBF

Figure 5: Result of proposed method for PD weighted MR image (a) Noiseless image (b) Noisy Image (c) Output image by IDEAHBF

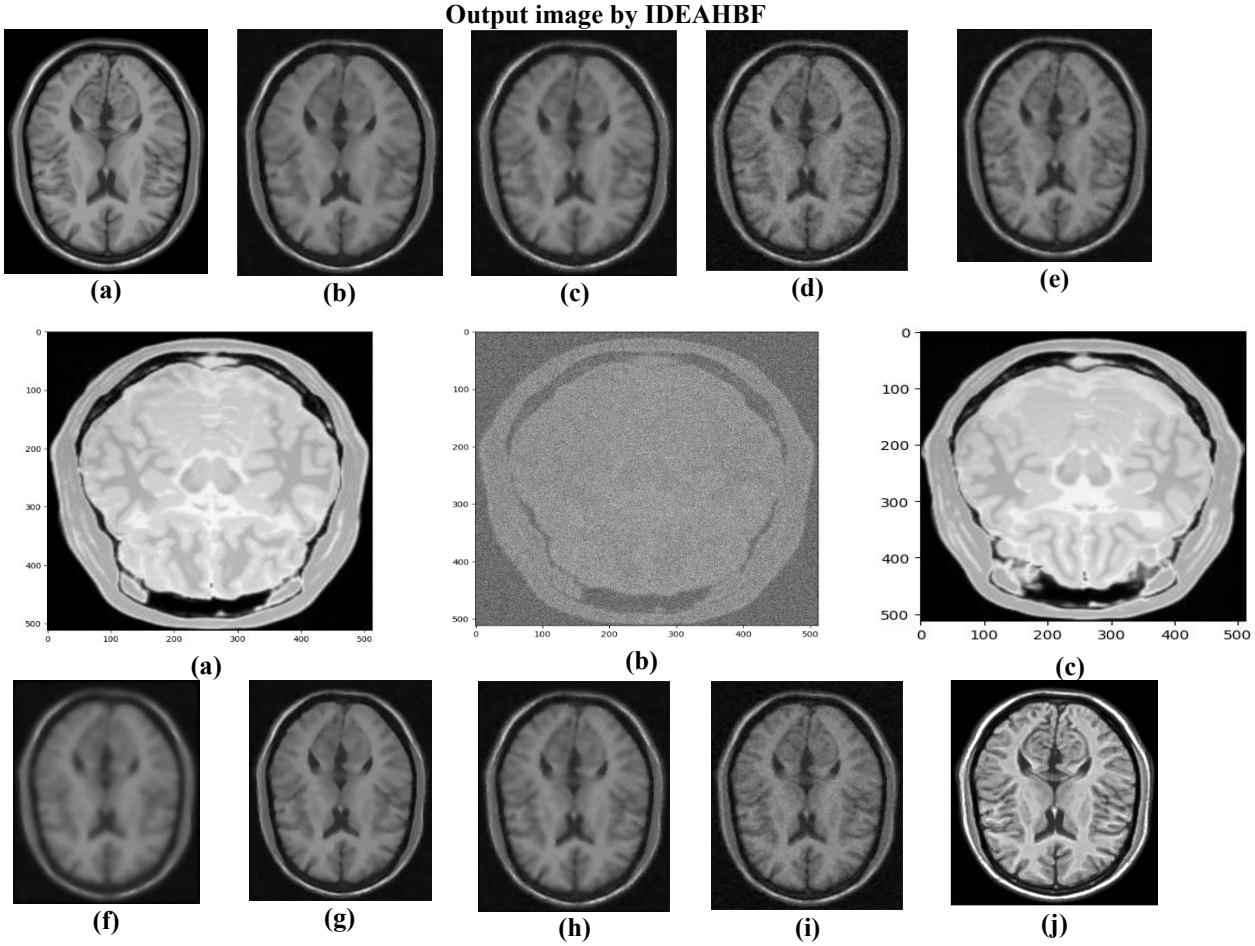

Figure 6: The output pictures acquired by the proposed method and other ways that already exist for T1 weighted MR image where (a) FPDE[18], (b) NLM [23], (c) WF [21], (d) MCD [16], (e) TV [14], (f) ADMF [20], (g) MCR [22], (h) ADF [15], (i) Gabor [6] and (j) Proposed IDAEHBF

Quantitative assessment:

The performance of the proposed IDAEHBF has been assessed with the aid of quantitative analysis. It judges and compares the proposed method's efficacy with other existing methods in terms of numeric value. The values are obtained by implementing the performance assessment parameters as mentioned in section 4. The quantifiable analysis has been calculated for the entire images of dataset. The comparative quantitative includes the results of FPDE[18], NLM [23], WF [21], MCD [16], TV [14], ADMF [20], MCR [22], ADF [15] and Gabor [6] filters which is reported in literature.

Table 3, 4 and 5 demonstrate the comparative numerical evaluation between the proposed and other existing methods for T1, T2 and PD brain respectively. It includes the performance assessments parameters of FRAP, HVSAP, and NRAP respectively. From the Table 3, the values of metrics such as MSE, PSNR, CP, NAE, UQI and SSIM and PSI have the following numeric scores of the proposed method 0.0227, 63.4917, 0.9465, 0.7429, 0.4423, 0.7242 and 0.6752 respectively. Tables 4 shows the comparative quantitative result for the entire images of 9% noise variance of T2 dataset with the following values MSE, PSNR, CP, NAE, UQI, SSIM and PSI respectively 0.0337, 67.8120, 0.9439, 0.9332, 0.6418, 0.0.4923 and 0.6782 respectively. Table 5 shows the quantitative result of PD MRI images. The numeric values of MSE, PSNR, CP, NAE, UQI, SSIM and PSI are 0.0551, 65.2952, 0.9432, 0.8991, 0.8592, 0.5395 and 0.8954 respectively. The comparative graphic line plot of Table 3, 4 and 5 is illustrated by Figure 7, 8 and 9 respectively.

Table 3: Comparative quantitative evaluation amid the reported methods and proposed IDAEHBF for T1 Brain MR image with 9% noise variance

Methods	Parameters						
	MSE	PSNR	SSIM	UQI	CP	NAE	PSI
FPDE[18]	0.4603	35.6897	0.7394	0.7314	0.4622	0.7236	0.314
NLM [23]	0.5713	37.2431	0.72521	0.7121	0.4523	0.7762	0.4215
WF [21]	0.6213	33.9214	0.7424	0.7245	0.4432	0.7923	0.4682
MCD [16]	0.5413	37.5215	0.81351	0.7931	0.4332	0.5345	0.3213
TV [14]	0.7932	32.1251	0.7215	0.7347	0.4454	0.7632	0.4632
ADMF [20]	0.7927	31.2351	0.7825	0.7281	0.4532	0.7792	0.4627
MCR [22]	0.6942	31.3251	0.7336	0.7267	0.4789	0.7823	0.3829
ADF [15]	0.8231	29.2541	0.8126	0.7512	0.5128	0.7154	0.4820
Gabor [6]	0.1638	61.3452	0.8734	0.9123	0.6347	0.5132	0.5728
Proposed	0.0337	67.8120	0.9439	0.9332	0.6418	0.4923	0.6782

Table 4: Comparative quantitative evaluation amid the reported methods and proposed IDAEHBF for T2 Brain MR image with 9% noise variance

Methods	Parameters						
	MSE	PSNR	SSIM	UQI	CP	NAE	PSI
FPDE[18]	0.6959	38.5121	0.7932	0.5725	0.4721	0.8125	0.4789
NLM [23]	0.6923	38.2925	0.7987	0.5582	0.4697	0.8415	0.5629
WF [21]	0.5939	34.545	0.8051	0.5681	0.4645	0.8523	0.6351
MCD [16]	0.3251	45.6542	0.8123	0.5515	0.5097	0.7799	0.6692
TV [14]	0.3351	44.5191	0.7652	0.5219	0.4698	0.8498	0.7539
ADMF [20]	0.3259	43.8921	0.7753	0.5492	0.5489	0.6125	0.7792
MCR [22]	0.3315	44.6129	0.8949	0.5629	0.5792	0.6561	0.7159
ADF [15]	0.2519	47.9219	0.7859	0.6249	0.5395	0.7921	0.6295
Gabor [6]	0.0692	57.982	0.9124	0.7492	0.7742	0.5925	0.7215
Proposed	0.0551	65.2952	0.9432	0.8991	0.8592	0.5395	0.8954

Methods	**Parameters**						
	MSE	**PSNR**	**SSIM**	**UQI**	**CP**	**NAE**	**PSI**
FPDE[18]	**0.3210**	**27.1439**	**0.6352**	**0.4367**	**0.3092**	**0.7892**	**0.3762**
NLM [23]	**0.4792**	**24.156**	**0.6425**	**0.4527**	**0.3189**	**0.7712**	**0.3216**
WF [21]	**0.3287**	**26.5492**	**0.6782**	**0.4732**	**0.3026**	**0.7737**	**0.3792**
MCD [16]	**0.7921**	**22.456**	**0.6621**	**0.4623**	**0.3153**	**0.8032**	**0.3498**
TV [14]	**0.3162**	**24.1567**	**0.7254**	**0.4713**	**0.2915**	**0.7752**	**0.6725**
ADMF [20]	**0.3526**	**26.8927**	**0.7692**	**0.4727**	**0.3691**	**0.7052**	**0.3215**
MCR [22]	**0.5726**	**23.456**	**0.7689**	**0.5556**	**0.3793**	**0.7792**	**0.3494**
ADF [15]	**0.5826**	**23.2621**	**0.5142**	**0.5681**	**0.4013**	**0.7952**	**0.3215**
Gabor [6]	**0.0798**	**58.9215**	**0.9012**	**0.6628**	**0.3419**	**0.7654**	**0.6315**
Proposed	**0.0227**	**63.4917**	**0.9465**	**0.7429**	**0.4423**	**0.7245**	**0.6752**

Table 5: Comparative quantitative evaluation amid the reported methods and proposed IDAEHBF for PD Brain MR image with 9% noise variance

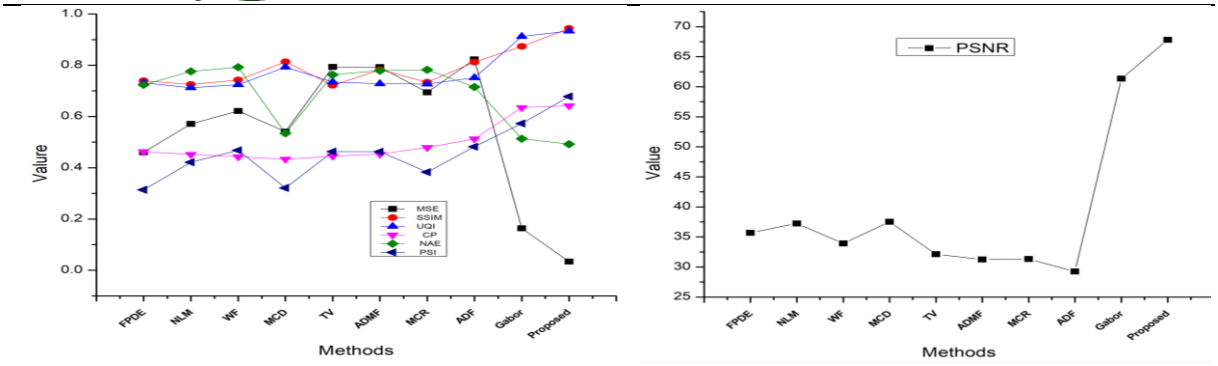

(a) (b)

Figure 7: Line plot comparing the variables in Table 3 with respect to T1 images (a) shows the values MSE, CP, NAE, UQI, SSIM and PSI respectively; (b) illustrates PSNR

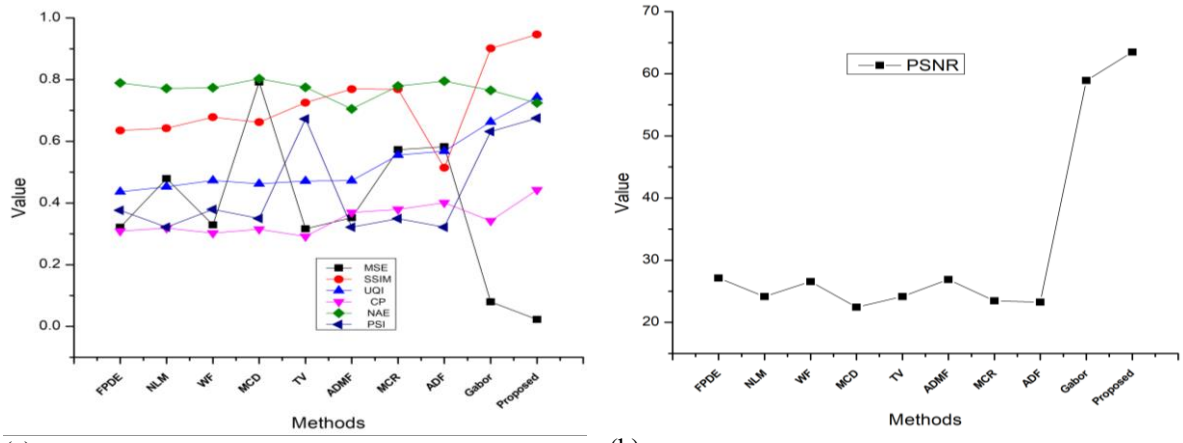

(a) (b)

Figure 8: Line plot comparing the variables in Table 4 with respect to T2 images (a) shows the values MSE, CP, NAE, UQI, SSIM and PSI respectively; (b) illustrates PSNR

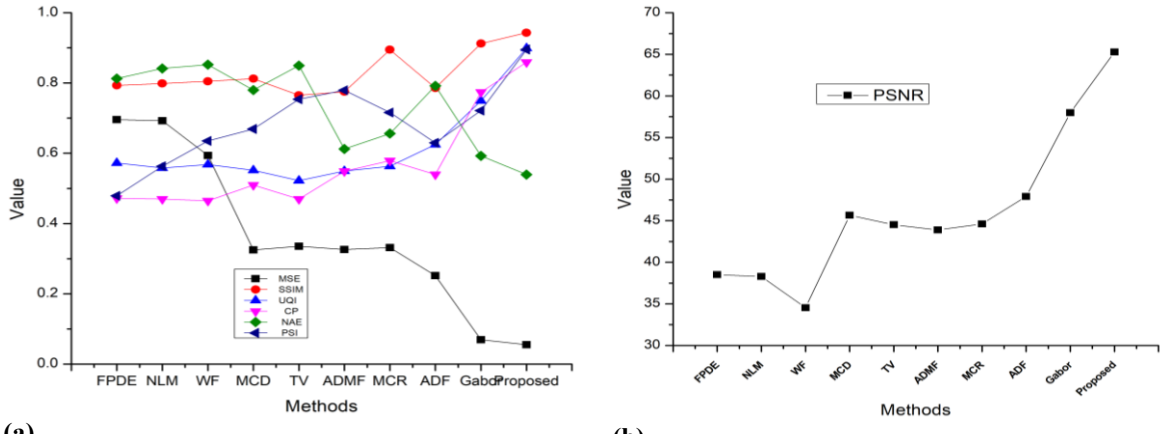

(a) **(b)**

Figure 9: Line plot comparing the variables in Table 5 with respect to TD images (a) shows the values MSE, CP, NAE, UQI, SSIM and PSI respectively; (b) illustrates PSNR;

The proposed method uses four encoding and decoding layers respectively. The encoding layers reduce all the data and to a single neuron and then the decoding layers use up sampling to increase the data in the model. This process removes the noise in the images and ensures that only the important data remains. The proposed IDAEHBF has been trained for 100 epochs. Figure 10 shows a graphical plot of PSNR vs number of epoch. The graph shows the variation PSNR values while increasing the epoch during training of the model.

DOI: 10.5123/inj.2023.4.in82
ISSN:2093-4777 | E-ISSN:2093-6931
Vol. 27 Iss. 4 (2023)

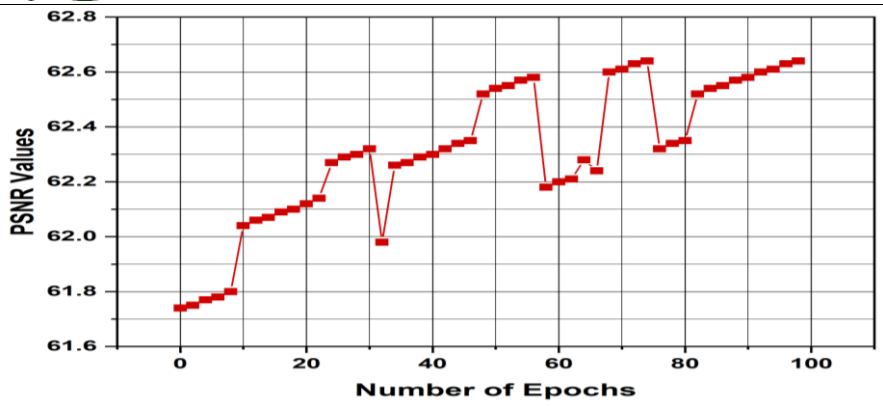

Figure 10: Plot of number of epochs vs PSNR

Conclusion

The primarily objective of the present work was to restore, denoise and enhance the brain MRI images which is usually affected by Rician noise. The objective was accomplished with the aid of the proposed improved denoising auto encoder deep learning based high boost filter (IDAEHBF). The IDAEHBF combines the attributes of conventional denoising auto encoder (CDAE) and high boost filter (HBF). The following modification had been implemented in order to the develop the IDAEHBF. It was begun with the implementation of IDEA where the CDAE was clubbed with the symmetric skip connection between the layers of encoder and decoder. It helps to reduce the issues of gradient flow, multi-scale feature learning and mitigating information loss. Furthermore, the IDEA was clubbed with HBF where the IDEA provides a better reconstructed denoised image as an alternative of conventional approach. Thus, both the modifications deliver a single framework for restoration, denoising and enhancement of brain MRI images instead of performing separately.

The performance of the proposed IDAEHBF was measured on the 9% noise variance of T1, T2 and PD brain image respectively. The dataset was collected from the Brain web MRI database. The performance was demonstrated in terms of qualitative as well as quantitative study. The qualitative study was used to exemplify the improvement in image quality which was obtained by the proposed IDAEHBF. Furthermore, the quantitative study was articulated with respect to the metrics of FRAP, HVSAP, and NRAP to measure the efficiency of the proposed IDAEHBF. The metrics like MSE, PSNR, CP, and NAE were employed as FRAP. UQI and SSIM were utilized as the parameters of HVSAP. The NRAP assessments parameters was cast-off in terms of PSI. Moreover, the performance of the proposed IDAEHBF was also presented in the form of comparative study. The existing methods like FPDE[18], NLM [23], WF [21], MCD [16], TV [14], ADMF [20], MCR [22], ADF [15] and Gabor [6] were used for the comparative study. Based on both qualitative and quantitative studies, it has been found that the suggested IDAEHBF is the best way to restore, denoise, and improve MRI images with Rician noise while keeping their edges and boundaries. The IDAEHBF's results can be used to find the area of interest for image segmentation as well as to improve the accuracy of the feature extraction and classification processes.

References

1. C.R. Madan, Advances in studying brain morphology: The benefits of open-access data, Front. Hum. Neurosci. 11 (2017) 405.
2. [2] A. Griffa, P.S. Baumann, J.-P. Thiran, P. Hagmann, Structural connectomics in brain diseases, Neuroimage. 80 (2013) 515–526.
3. [3] J.C. Richardson, R.W. Bowtell, K. Mäder, C.D. Melia, Pharmaceutical applications of magnetic resonance imaging (MRI), Adv. Drug Deliv. Rev. 57 (2005) 1191–1209.
4. [4] H.M. Golshan, R.P.R. Hasanzadeh, A modified Rician LMMSE estimator for the restoration of magnitude MR images, Optik (Stuttg). 124 (2013) 2387–2392. https://doi.org/10.1016/j.ijleo.2012.07.001.
5. [5] Z.-P. Liang, P.C. Lauterbur, Principles of magnetic resonance imaging, SPIE Optical Engineering Press Bellingham, 2000.
6. [6] V. Kumar, S. Srivastava, Performance analysis of reshaped Gabor filter for removing the Rician distributed noise in brain MR images, Proc. Inst. Mech. Eng. Part H J. Eng. Med. 236 (2022) 1216–1231.
7. [7] R.B. Yadav, S. Srivastava, R. Srivastava, A partial differential equation-based general framework adapted to Rayleigh's, Rician's and Gaussian's distributed noise for restoration and

enhancement of magnetic resonance image, J. Med. Phys. 41 (2016) 254.
8. [8] P. Vincent, Denoising autoencoder.pdf, Icml. (2008).
9. [9] R. Srivastava, J.R.P. Gupta, H. Parthasarthy, S. Srivastava, PDE based unsharp masking, crispening and high boost filtering of digital images, Commun. Comput. Inf. Sci. 40 (2009) 8–13. https://doi.org/10.1007/978-3-642-03547-0_2.
10. [10] X.-J. Mao, C. Shen, Y.-B. Yang, Image Restoration Using Convolutional Auto-encoders with Symmetric Skip Connections, (2016) 1–17. http://arxiv.org/abs/1606.08921.
11. [11] J. Mohan, V. Krishnaveni, Y. Guo, A survey on the magnetic resonance image denoising methods, Biomed. Signal Process. Control. 9 (2014) 56–69. https://doi.org/10.1016/j.bspc.2013.10.007.
12. [12] P. Coupé, J. V. Manjón, E. Gedamu, D. Arnold, M. Robles, D.L. Collins, Robust Rician noise estimation for MR images, Med. Image Anal. 14 (2010) 483–493. https://doi.org/10.1016/j.media.2010.03.001.
13. [13] J. Lu, J. Tian, L. Shen, Q. Jiang, X. Zeng, Y. Zou, Rician Noise Removal via a Learned Dictionary, Math. Probl. Eng. 2019 (2019). https://doi.org/10.1155/2019/8535206.
14. [14] B. Zhang, X. Wang, Y. Li, Z. Zhu, A new di ff erence of anisotropic and isotropic total variation regularization method for image restoration, 20 (2023) 14777–14792.
15. [15] R.R. Kumar, A. Kumar, S. Srivastava, Anisotropic Diffusion Based Unsharp Masking and Crispening for Denoising and Enhancement of MRI Images, 2020 Int. Conf. Emerg. Front. Electr. Electron. Technol. ICEFEET 2020. (2020) 0–5. https://doi.org/10.1109/ICEFEET49149.2020.9186966.
16. [16] R. Srivastava, S. Srivastava, R.B. Yadav, Modified complex diffusion based nonlinear filter for restoration and enhancement of magnetic resonance images, Int. J. Biomed. Eng. Technol. 23 (2017) 19. https://doi.org/10.1504/ijbet.2017.10003042.
17. [17] P. Kumar, S. Srivastava, Y. Padma Sai, Recasted nonlinear complex diffusion method for removal of Rician noise from breast MRI images, J. Def. Model. Simul. (2021) 15485129211052284.
18. [18] R.B. Yadav, S. Srivastava, R. Srivastava, An efficient PDE-Based nonlinear filter adapted to Rician noise for restoration and enhancement of magnetic resonance images, India Int. Conf. Inf. Process. IICIP 2016 - Proc. (2017) 0–4. https://doi.org/10.1109/IICIP.2016.7975339.
19. [19] D. Lee, C.S. Yun, S.H. Kang, M. Park, Y. Lee, Performance evaluation of 3D median modified Wiener filter in brain T1-weighted magnetic resonance imaging, Nucl. Instruments Methods Phys. Res. Sect. A Accel. Spectrometers, Detect. Assoc. Equip. 1047 (2023) 167779. https://doi.org/10.1016/j.nima.2022.167779.
20. [20] M. Redhya, K. Sathesh Kumar, Refining PD classification through ensemble bionic machine learning architecture with adaptive threshold based image denoising, Biomed. Signal Process. Control. 85 (2023) 104870. https://doi.org/10.1016/j.bspc.2023.104870.
21. [21] K. Singh, R. Kumar, BRAIN MRI IMAGE DENOISING USING FILTERING APPROACHES, (n.d.).
22. [22] K. Ali, A.N. Qureshi, M.S. Bhatti, A. Sohail, M. Hijji, A. Saeed, De-Noising Brain MRI Images by Mixing Concatenation and Residual Learning (MCR), Comput. Syst. Sci. Eng. 45 (2023) 1167–1186. https://doi.org/10.32604/csse.2023.032508.
23. [23] P. Thakur, N. Syamala, Y. Karuna, S. Saritha, Performance Analysis of IIC techniques for Brain MR-images, Proc. 10th Int. Conf. Signal Process. Integr. Networks, SPIN 2023. (2023) 351–357. https://doi.org/10.1109/SPIN57001.2023.10116089.
24. [24] S. Kollem, K.R. Reddy, D.S. Rao, A novel diffusivity function-based image denoising for MRI medical images, Multimed. Tools Appl. (2023). https://doi.org/10.1007/s11042-023-14457-3.
25. [25] P.H. Dinh, A Novel Approach Based on Marine Predators Algorithm for Medical Image Enhancement, Sens. Imaging. 24 (2023). https://doi.org/10.1007/s11220-023-00411-y.
26. [26] C.A. Cocosco, Brainweb: Online interface to a 3D MRI simulated brain database, Neuroimage. 5 (1997).
27. [27] R. Srivastava, S. Srivastava, R.B. Yadav, Identification and removal of different categories of noises from magnetic resonance image using hybrid partial differential equation-based filter, Int. J. Digit. Signals Smart Syst. 1 (2017) 87. https://doi.org/10.1504/ijdsss.2017.10008982.
28. [28] S. Sridhar, Digital Image Processing, OUP India, 2011. https://books.google.co.in/books?id=hWAyngEACAAJ.
29. [29] A. Kumar, S. Srivastava, Restoration and enhancement of breast ultrasound images using extended complex diffusion based unsharp masking, Proc. Inst. Mech. Eng. Part H J. Eng. Med. (2021) 09544119211039317.
30. [30] A. Kumar, P. Kumar, S. Srivastava, A skewness reformed complex diffusion based unsharp masking for the restoration and enhancement of Poisson noise corrupted mammograms, Biomed. Signal Process. Control. 73 (2022) 103421. https://doi.org/10.1016/j.bspc.2021.103421.

ISSN:2093-4777 | E-ISSN:2093-6931
DOI: 10.5123/inj.2023.4.in82
Vol. 27 Iss. 4 (2023)